DOI: 10.1002/anie.201309306

Pigment Design

Full-Spectrum Photonic Pigments with Non-iridescent Structural Colors through Colloidal Assembly**

*Jin-Gyu Park, Shin-Hyun Kim, Sofia Magkiriadou, Tae Min Choi, Young-Seok Kim, and Vinothan N. Manoharan**

Abstract: *Structurally colored materials could potentially replace dyes and pigments in many applications, but it is challenging to fabricate structural colors that mimic the appearance of absorbing pigments. We demonstrate the microfluidic fabrication of "photonic pigments" consisting of microcapsules containing dense amorphous packings of core–shell colloidal particles. These microcapsules show non-iridescent structural colors that are independent of viewing angle, a critical requirement for applications such as displays or coatings. We show that the design of the microcapsules facilitates the suppression of incoherent and multiple scattering, enabling the fabrication of photonic pigments with colors spanning the visible spectrum. Our findings should provide new insights into the design and synthesis of materials with structural colors.*

Coloration free from chemical- or photo-bleaching is a central goal in paints, cosmetics, and information displays. Such long-lasting colors can be achieved with non-absorbing nanostructures that selectively reflect light of certain wavelengths through constructive interference. This phenomenon is called structural coloration.[1] Colloidal suspensions are ideal for making structurally colored materials, as they are inexpensive, they can be dynamically manipulated with external fields,[2] and they have optical properties that can be tuned through synthesis, morphology, and the suspension medium.[3] The primary motivation for our work is the production of colloid-based photonic pigments that can be used for highly efficient reflective displays. Grayscale, field-addressable electronic-ink-type displays have been produced from microcapsule pigments containing black colloidal particles that absorb light and white particles that scatter light.[4] Full-color reflective displays require pigments that reflect light efficiently and isotropically, so that the color does not vary with the viewing angle. In principle, such colors can be produced from amorphous packings of colloidal particles,[5] which do not suffer from the angle-dependence, or iridescence, of the crystalline colloidal packings that have been the subject of many previously reported photonic pigment schemes.[6] However, processes for synthesizing large quantities of photonic pigments based on amorphous colloidal packings are only beginning to emerge.[7–9]

The principal challenge of making isotropic structural coloration through colloidal assembly is control over incoherent and multiple scattering. Previous approaches produce bulk coatings of colloidal particles a few micrometers thick, corresponding roughly to the extinction length of the nanostructures. If the sample is too thick, white color from multiple scattering dominates, compromising color saturation.[8] Furthermore, as the size of the colloidal particles increases, the structural resonance is compromised by incoherent scattering at shorter wavelengths.[9] Therefore, control over both incoherent and multiple scattering is necessary to realize photonic pigments with pronounced structural colors that cover the visible range. Another technical challenge lies in making the amorphous nanostructures. Charged nanoparticles tend to crystallize as the concentration increases.[10] Alternatives to avoid crystallization are to use bidisperse suspensions,[8,9] cohesive particles,[11] or fast drying in the presence of salts;[12] but such routes complicate the processing.

Herein, we present a new colloidal assembly method to fabricate microencapsulated photonic pigments that cover the full spectrum with little multiple scattering. The key to our approach is a design with three structural length scales: the scatterer size, the inter-scatterer distance, and the capsule size. We used microfluidic techniques to produce spherical microcapsules of approximately 100 μm in diameter, which contain densely packed, amorphous arrays of colloidal particles. The encapsulated particles are polystyrene/poly(*N*-isopropylacrylamide-*co*-acrylic-acid) (PS/poly(NiPAm-AAc)) core–shell particles with shells that are closely index-matched to the surrounding water. As shown in our previous work,[13] the use of core–shell particles allows us to independently tune the scattering of the particles, which is set by the core size, and the wavelength of the structural resonance, which is controlled by the shell diameter. Thus, the core

[*] Dr. J.-G. Park, S. Magkiriadou, Prof. V. N. Manoharan
School of Engineering and Applied Sciences and Department of Physics, Harvard University,17 Oxford St.
Cambridge, MA 02138 (USA)
E-mail: vnm@seas.harvard.edu
Homepage: http://manoharan.seas.harvard.edu
Prof. S.-H. Kim, T. M. Choi
Department of Chemical and Biomolecular Engineering, Korea Advanced Institute of Science and Technology
Daejeon, 305-701 (Korea)
Dr. Y.-S. Kim
Korea Electronics Technology Institute, 68 Yatap-dong
Bundang-gu, Seongnam-si, Gyeonggi-do (Korea)

[**] This research is supported by an International Collaboration grant (Sunjin-2010-002) from the Ministry of Trade, Industry & Energy of Korea. We also acknowledge support from the Harvard MRSEC through the NSF (DMR-0820484). This work is performed in part at the Center for Nanoscale Systems (CNS) at Harvard University, which is supported by the National Science Foundation (ECS-0335765). We also thank Prof. Gi-Ra Yi from Sungkyunkwan University for helpful discussions.

Supporting information for this article is available on the WWW under http://dx.doi.org/10.1002/anie.201309306.

particles, which dominate the scattering, can be small compared to the shells. In this case, the capsules have weak incoherent and multiple scattering. The coherent scattering responsible for structural color dominates, and we are able to make photonic pigments with isotropic structural colors throughout the visible range.

We made these pigments using a microfluidic technique. We started with an aqueous suspension of PS/poly(NiPAm-AAc) core–shell particles synthesized through seeded emulsion polymerization,[14] using PS nanoparticles with a hydrodynamic radius ($R_{h,PS}$) of 78 ± 5 nm as seeds. The ratio of NiPAm monomer to seed particle, which controls the thickness of the soft poly(NiPAm) shell, was 0.5% w/w, which yielded a core–shell hydrodynamic radius ($R_{h,core-shell}$) of 168 ± 17 nm. We matched the refractive index of the shell to that of the suspension medium by copolymerizing 4.0% w/w acrylic acid (AAc) in the poly(NiPAm) shell. We then encapsulated this suspension ($\phi_{core-shell} \approx 0.28$) in the innermost phase of water-in-oil-in-water (W/O/W) double-emulsion droplets using a capillary microfluidic device, as shown in Figure 1a.[15] The aqueous suspension and an oil phase containing a UV-curable monomer, ethoxylated trimethylolpropane triacrylate (ETPTA), were simultaneously injected through a hydrophobic capillary, creating a train of suspension droplets in the continuous monomer flow. The hydrophobicity of the capillary prevented the droplets from wetting. This core–sheath was then emulsified into the continuous phase, aqueous poly(vinyl alcohol) (PVA; 10% w/w), at the tip of the capillary, yielding W/O/W double-emulsion drops where the innermost phase was the particle suspension and the middle phase an ultra-thin shell of oil, as shown in Figure 1b. These droplets were the precursors to our photonic microcapsules.

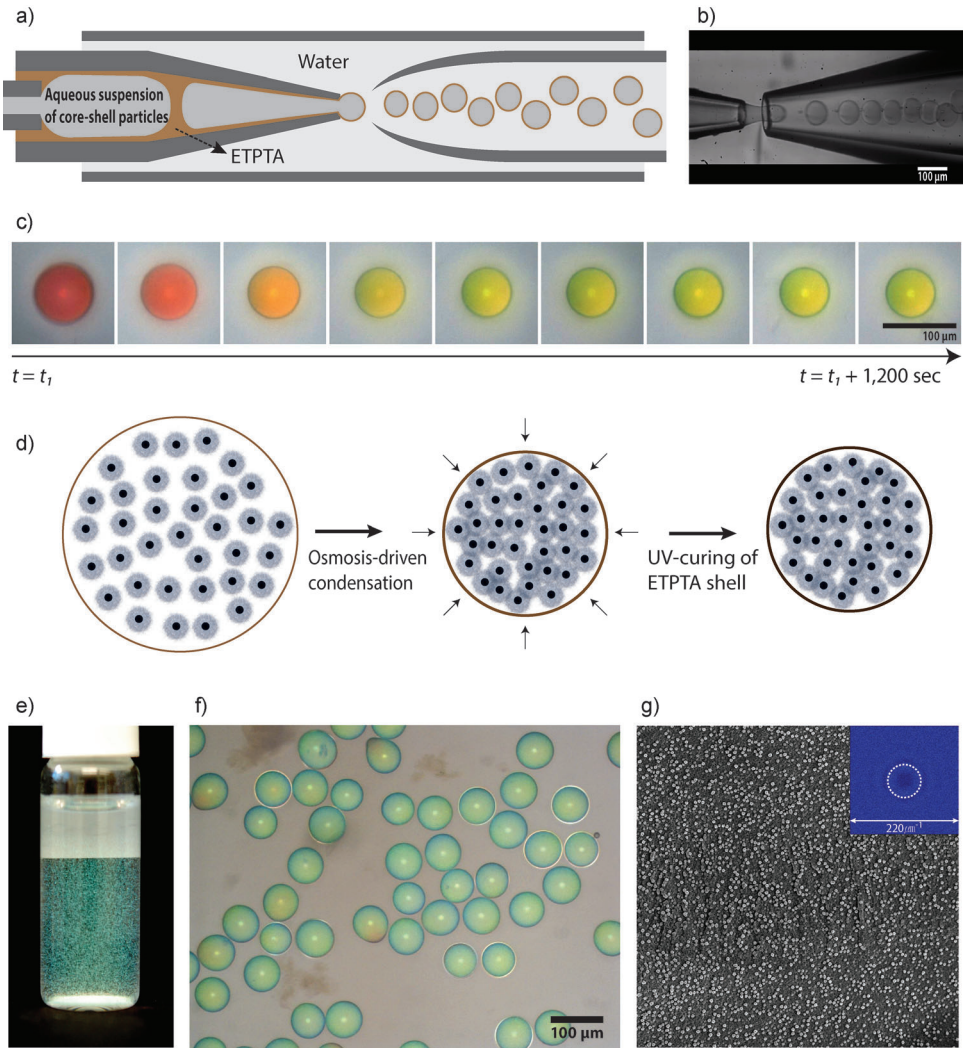

Figure 1. Fabrication of photonic pigments. a) Schematic of a capillary microfluidic device for the production of W/O/W double-emulsion droplets with a thin ethoxylated trimethylolpropane triacrylate (ETPTA) membrane. b) Optical micrograph showing generation of uniform W/O/W droplets. The innermost phase contains an aqueous suspension of core–shell particles with a volume fraction ($\phi_{core-shell}$) of ca. 0.28. c) Time-series optical micrographs of osmosis-driven condensation of droplets at 340 mOsm L^{-1}, where t_1, the elapsed time for microscope analysis, is ca. 5 min. d) Schematic of the structure of particles during osmosis-driven condensation. e,f) A photograph and an optical micrograph of the photonic pigments in water after UV-curing of the ETPTA shell. The sample is compressed at 440 mOsm L^{-1}. A few capsules show yellow spots due to local deformation of the polymer shell. g) Scanning electron micrograph of a cross-section of a cryogenically fractured photonic pigment microcapsule prepared under compression at 440 mOsm L^{-1}. The field of view is 20.0 µm wide. The inset in (g) is the two-dimensional Fourier power spectrum derived from (g).

The precursor droplets are designed to facilitate the preparation of amorphous nanostructures. The double emulsion makes it possible to concentrate the suspension by an osmotic pressure gradient.[16] Furthermore, the softness of the particle shells inhibits crystallization during concentration.[17] We concentrated the particles by placing the W/O/W droplets into an aqueous solution of PVA and sodium chloride (NaCl), creating a positive osmotic pressure difference that forced the water out through the thin ETPTA membrane and caused the droplets to shrink isotropically, as shown in Figure 1c. As the droplets shrank, they developed color that blue-shifted with increasing concentration (Figure 1c). We then polymerized the ETPTA layer by exposing it to ultraviolet (UV) light for

30 seconds, as illustrated in Figure 1d. The ETPTA layer ($n_{ETPTA} = 1.4689$) yields a 0.8 μm-thick, optically transparent shell after curing. The resulting microcapsules are monodisperse and display non-iridescent structural colors, as shown in Figure 1e,f.

The internal structure of these photonic pigments is random and isotropic, as shown by scanning electron microscope images of cryogenically fractured microcapsules (Figure 1g; see also the Supporting Information, Figure S1a). Two-dimensional Fourier analysis of a 20 μm × 20 μm cross-section of microcapsule shows a ring pattern (Figure 1g), indicating that the structure is isotropic. We observed a peak corresponding to a length scale of 0.217 μm, which is denoted by the dotted circle in the inset of Figure 1g.

We can control the colors by changing the average distance between the PS cores, which are the primary scatterers. The inter-scatterer distance is controlled by the degree of droplet compression, which depends on the osmotic pressure difference used to concentrate the particles. For example, we can prepare red microcapsules at 180 mOsm L^{-1}, yellow at 260 mOsm L^{-1}, and green at 440 mOsm L^{-1}. At each osmolarity, we incubated emulsion droplets containing core–shell particles with $R_{h,core-shell} = 168 \pm 17$ nm for two hours to equilibrate the osmotic pressure before we polymerized the ETPTA shell. Reflectance spectra of the resulting microcapsules (Figure 2a) show that the characteristic peak shifts from 610 nm to 550 nm as the osmotic pressure increases, but the normalized full width at half-maximum, $\Delta\lambda/\lambda_{max}$, remains almost constant (Figure 2b).

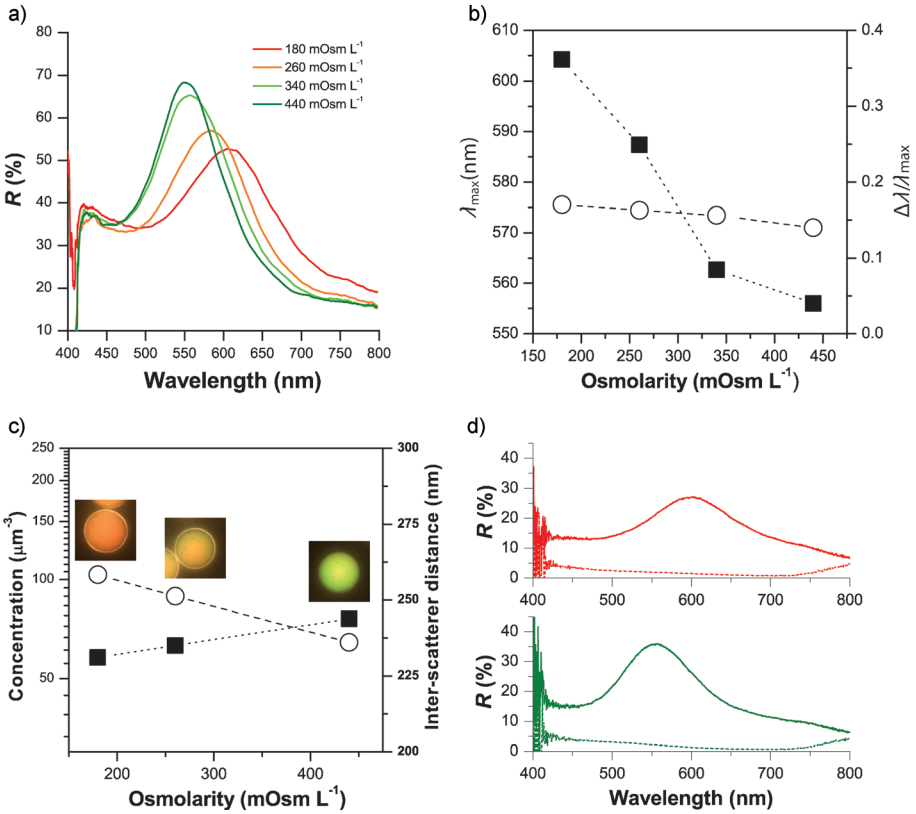

Figure 2. Control of structural colors through osmotic pressure. a) Reflectance spectra of the microcapsules equilibrated under different osmotic pressures. b) Plots of peak positions (dark squares) and normalized full-width at half maximum (FWHM; open circles) of the microcapsules as a function of osmotic pressure. c) Estimated concentration of PS scatterers (dark squares) and average spacing between PS scatterers (open circles) as a function of osmotic pressure. Insets are bright-field (reflection) optical micrographs of red, yellow, and green microcapsules prepared under 180 mOsm L^{-1}, 260 mOsm L^{-1}, and 440 mOsm L^{-1}, respectively. The field of view for the insets is 100 μm wide. d) Co-polarization (lines) and cross-polarization (dots) reflection spectra of red (upper) and green (lower) photonic microcapsules.

We can estimate the inter-scatterer distance (d) from the reflection spectra. If the particles inside the microcapsules are packed amorphously, and we assume back-reflected light, then

$$d = 0.6\lambda/n_{medium} \quad (1)$$

where λ is the resonant wavelength and n_{medium} is the effective refractive index of the medium,[18] which depends on the volume fraction of the PS cores.[13] Equation (1) assumes that the average spacing between particles is determined by the first peak of the structure factor of colloidal glasses at similar densities.[19] Because we do not know a priori the volume fraction of polystyrene, we calculated d using an iterative process (see the Supporting Information). From this calculation, we determined the number density of PS scatterers and the average distance between them as a function of osmotic pressure (Figure 2c). We find that, for the green microcapsules, the inter-scatterer distance calculated from the spectrum (236 nm) agrees well with that obtained through Fourier analysis of an SEM image of the same sample (217 ± 14 nm). On the basis of the spectra, calculations, and SEM analysis, we conclude that the particles are compressed into roughly 35% of their original volume at 440 mOsm L^{-1}.

In all of these samples, coherent scattering on resonance dominates background scattering off resonance. We characterized the background by the intensity at short wavelengths (420–435 nm), where the reflectance has the highest value off-resonance. This background arises from incoherent scattering from individual particles and multiple scattering. The ratio of the peak intensity to background ($I_{max}/I_{background}$) increases from 1.35 for red photonic microcapsules to 1.83 for green ones (Figure 2a). This quantity is one measure of the color saturation: the lower the value, the whiter the sample, owing to mixing of the resonant color with incoherently scattered blue light. Although the off-resonant incoherent scattering is

not negligible, particularly for red microcapsules, it is significantly smaller than the resonant contribution for all the samples.

We isolated the contribution of multiply scattered light to the incoherent scattering by measuring the polarization dependence of the reflection spectra, because multiply scattered light loses memory of its original polarization. We linearly polarized the incident light and placed another linear polarizer in front of the detector (Figure S2). Under co-polarization, we observed spectral peaks at approximately 560 nm for green and 600 nm for red microcapsules (Figure 2d), whereas the cross-polarized spectra for both samples are nearly flat. From these measurements we calculated the ratio of singly to multiply scattered light at the resonant wavelength, assuming that the cross-polarized signal is due to multiple scattering and that the contribution of multiple scattering to the signal is the same in both the co- and cross-polarized spectra. We find values of 16.2 for green and 17.3 for red microcapsules, which indicate that multiple scattering does not contribute significantly to the color. We also calculated the contribution of multiple scattering to the background from the average reflectivity through crossed (I_{cr}) and parallel (I_{co}) polarizers at short wavelengths (420–435 nm), $I_{cross}/(I_{co}+I_{cross})$. We find that multiple scattering accounts for only 23% of the background intensity in green and 24% in red microcapsules, thus indicating that the primary source of background scattering is incoherent single scattering from PS core particles. From these measurements, we conclude that multiple scattering does not compromise the color saturation in our system, in contrast to other systems with isotropic structural colors where multiple scattering has to be suppressed through absorption.[7,8,10]

To complete the full color spectrum, we made microcapsules from core–shell particles of different sizes. We used the same osmotic compression and cores for all samples, so that the inter-scatterer distance was controlled by the thickness of the particle shells. We obtained photonic microcapsules with $R_{h,core\text{–}shell} = 135 \pm 24$ nm, green with $R_{h,core\text{–}shell} = 168 \pm 17$ nm, and red with $R_{h,core\text{–}shell} = 210 \pm 15$ nm, as shown in Figure 3.

The optical properties of our amorphous microcapsules are qualitatively different from those of crystalline structures, even for samples prepared with comparable particle sizes. For comparison, we prepared crystalline photonic supraballs with a diameter of about 90 μm through consolidation of 250 nm PS spheres in W/O droplets.[20] Reflection optical micrographs (Figure 4a,b) show the dramatic differences between the two samples: the amorphous microcapsules show colors that are uniform across each capsule and from capsule to capsule, whereas the crystalline supraballs show patches of different colors and variations between supraballs. To quantify these differences, we measured the spectra of single microcapsules and crystalline supraballs as a function of position (x) with a microscope-mounted, fiber-optic spectrometer (Figure 4c). The position of the spectral peak remains constant for the microcapsule (Figure 4d), whereas in the crystalline supraball it shifts by 40 nm or more (Figure 4e). This behavior arises from the anisotropy of the crystal, which leads to a variation in the resonant condition with angle. At the same time, the incompatibility of crystalline order with the spherical symmetry of the droplet likely leads to the formation of grain boundaries, which would account for the variation in colors from supraball to supraball. Our measurements highlight the

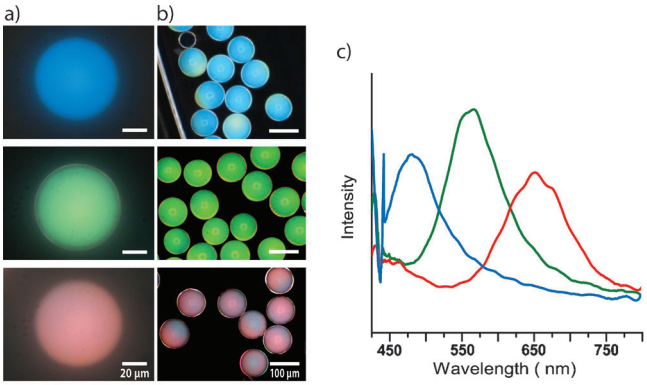

Figure 3. Photonic microcapsules with blue, green, and red structural colors prepared with different shell thicknesses of core–shell particles. a) Bright-field (reflection) and b) dark-field (reflection) optical micrographs of photonic microcapsules. c) Reflectance spectra of the microcapsules. All droplets are incubated at 440 mOsm L^{-1} for 1 h before ETPTA polymerization.

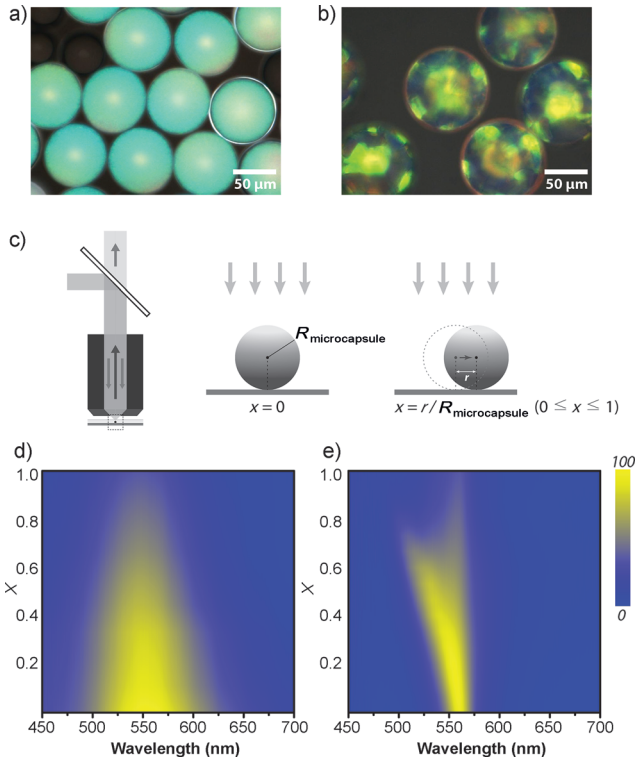

Figure 4. Photonic microcapsules show uniform structural color under different illumination directions. Bright-field (reflection) optical micrographs of a) photonic microcapsules and b) crystalline supraballs. c) Schematic of the apparatus used to measure the reflection spectra of a single microcapsule or supraball. d,e) Reflectivity (yellow: 100%, blue: 0%) of a microcapsule (d) and a crystalline supraball (e) as a function of position (x), where $x = 0$ at the center and $x = 1$ at the edge.

trade-off in optical performance between crystalline and isotropic structures: although the crystalline supraball has sharper resonant peaks at some locations, the isotropic microcapsule shows a broader, but more consistent, peak across a wide range of positions. We also measured the reflectivity of the microcapsules at various angles by rotating the sample stage. As shown in Figure S3a, the peak moves less than 10 nm and is independent of the viewing angle. Plots of $\Delta\lambda/\lambda_{max}$ as a function of angle in Figure S3b confirm that the optical properties of our microcapsules are independent of orientation.

In conclusion, we have demonstrated a new colloidal assembly method to fabricate photonic microcapsules with non-iridescent structural colors that cover the entire visible range. The length scales of our system are tuned to suppress multiple scattering, so that coherent scattering is the dominant process determining the color. We note that our system is optimized for structural inks that remain in a fluid medium. Pigments than can be dried might be made using a more rigid microcapsule. Another challenge is to increase the saturation across the visible range; as our experiments show, red microcapsules are not as saturated as green or blue ones owing to incoherent single scattering at short wavelengths. Our system provides several potential ways to reduce incoherent scattering; for example, one could vary the refractive indices of the core and shell, or optimize the ratio of the core size to the inter-particle spacing. The ability to independently tune refractive indices and length scales to optimize the color—all while maintaining the ability to form amorphous packings—make this a promising system for mass-produced photonic pigments.

Received: October 24, 2013
Revised: December 9, 2013
Published online: February 12, 2014

Keywords: colloids · dyes/pigments · isotropic structure · microfluidics · structural colors

[1] a) R. O. Prum, R. H. Torres, S. Williamson, J. Dyck, *Nature* **1998**, *396*, 28 – 29; b) P. Vukusic, J. R. Sambles, *Nature* **2003**, *424*, 852 – 855; c) S. Kinoshita, S. Yoshioka, *ChemPhysChem* **2005**, *6*, 1442 – 1459; d) M. D. Shawkey, S. L. Balenger, G. E. Hill, L. S. Johnson, A. J. Keyser, L. Siefferman, *J. R. Soc. Interface* **2006**, *3*, 527 – 532.

[2] a) R. C. Hayward, D. A. Saville, I. A. Aksay, *Nature* **2000**, *404*, 56 – 59; b) I. Muševič, M. Škarabot, U. Tkalec, M. Ravnik, S. Žumer, *Science* **2006**, *313*, 954 – 958; c) J. Ge, Y. Hu, Y. Yin, *Angew. Chem.* **2007**, *119*, 7572 – 7575; *Angew. Chem. Int. Ed.* **2007**, *46*, 7428 – 7431; d) J. D. Forster, J.-G. Park, M. Mittal, H. Noh, C. F. Schreck, C. S. O'Hern, H. Cao, E. M. Furst, E. R. Dufresne, *ACS Nano* **2011**, *5*, 6695 – 6700.

[3] a) J. F. Bertone, P. Jiang, K. S. Hwang, D. M. Mittleman, V. L. Colvin, *Phys. Rev. Lett.* **1999**, *83*, 300 – 303; b) M. L. Breen, A. D. Dinsmore, R. H. Pink, S. B. Qadri, B. R. Ratna, *Langmuir* **2001**, *17*, 903 – 907; c) C. Graf, D. L. J. Vossen, A. Imhof, A. van Blaaderen, *Langmuir* **2003**, *19*, 6693 – 6700.

[4] a) B. Comiskey, J. D. Albert, H. Yoshizawa, J. Jacobson, *Nature* **1998**, *394*, 253 – 255; b) T. Nisisako, T. Torii, T. Takahashi, Y. Takizawa, *Adv. Mater.* **2006**, *18*, 1152 – 1156.

[5] a) K. Ueno, A. Inaba, Y. Sano, M. Kondoh, M. Watanabe, *Chem. Commun.* **2009**, 3603 – 3605; b) M. Harun-Ur-Rashid, A. B. Imran, T. Seki, M. Ishii, H. Nakamura, Y. Takeoka, *ChemPhysChem* **2010**, *11*, 579 – 583.

[6] a) S.-H. Kim, S.-J. Jeon, G.-R. Yi, C.-J. Heo, J. H. Choi, S.-M. Yang, *Adv. Mater.* **2008**, *20*, 1649 – 1655; b) S.-H. Kim, S.-J. Jeon, S.-M. Yang, *J. Am. Chem. Soc.* **2008**, *130*, 6040 – 6046; c) S.-H. Kim, S.-J. Jeon, W. C. Jeong, H. S. Park, S.-M. Yang, *Adv. Mater.* **2008**, *20*, 4129 – 4134; d) T. Kanai, D. Lee, H. C. Shum, R. K. Shah, D. A. Weitz, *Adv. Mater.* **2010**, *22*, 4998 – 5002.

[7] Y. Takeoka, M. Honda, T. Seki, M. Ishii, H. Nakamura, *ACS Appl. Mater. Interfaces* **2009**, *1*, 982 – 986.

[8] J. D. Forster, H. Noh, S.-F. Liew, V. Saranathan, C. F. Schreck, L. Yang, J.-G. Park, R. O. Prum, S. G. J. Mochrie, C. S. O'Hern, H. Cao, E. R. Dufresne, *Adv. Mater.* **2010**, *22*, 2939 – 2944.

[9] Y. Takeoka, S. Yoshioka, A. Takano, S. Arai, K. Nueangnoraj, H. Nishihara, M. Teshima, Y. Ohtsuka, T. Seki, *Angew. Chem.* **2013**, *125*, 7402 – 7406; *Angew. Chem. Int. Ed.* **2013**, *52*, 7261 – 7265.

[10] a) P. Jiang, J. F. Bertone, K. S. Hwang, V. L. Colvin, *Chem. Mater.* **1999**, *11*, 2132 – 2140; b) O. D. Velev, A. M. Lenhoff, E. W. Kaler, *Science* **2000**, *287*, 2240 – 2243; c) D. J. Norris, E. G. Arlinghaus, L. Meng, R. Heiny, L. E. Scriven, *Adv. Mater.* **2004**, *16*, 1393 – 1399.

[11] Y. Gotoh, H. Suzuki, N. Kumano, T. Seki, K. Katagiri, Y. Takeoka, *New J. Chem.* **2012**, *36*, 2171 – 2175.

[12] Y. Takeoka, S. Yoshioka, M. Teshima, A. Takano, M. Harun-Ur-Rashid, T. Seki, *Sci. Rep.* **2013**, *50*, 2371 – 1 – 7.

[13] S. Magkiriadou, J.-G. Park, Y.-S. Kim, V. N. Manoharan, *Opt. Mater. Express* **2012**, *2*, 1343 – 1352.

[14] A. Perro, G. Meng, J. Fung, V. N. Manoharan, *Langmuir* **2009**, *25*, 11295 – 11298.

[15] S.-H. Kim, J. W. Kim, J.-C. Cho, D. A. Weitz, *Lab Chip* **2011**, *11*, 3162 – 3166.

[16] S.-H. Kim, J.-G. Park, T. M. Choi, V. N. Manoharan, D. A. Weitz, *Nat. Commun.* **2013**, *5*, 3068.

[17] J. Mattsson, H. M. Wyss, A. Fernandez-Nieves, K. Miyazaki, Z. Hu, D. R. Reichman, D. A. Weitz, *Nature* **2009**, *462*, 83 – 86.

[18] H. Noh, S.-F. Liew, V. Saranathan, R. O. Prum, S. G. J. Mochrie, E. R. Dufresne, H. Cao, *Opt. Express* **2010**, *18*, 11942 – 11948.

[19] R. Kurita, E. R. Weeks, *Phys. Rev. E* **2010**, *82*, 011403.

[20] S.-H. Kim, S. Y. Lee, G.-R. Yi, D. J. Pine, S.-M. Yang, *J. Am. Chem. Soc.* **2006**, *128*, 10897 – 10904.

